Synthesis and Characterization of Phthalocyanine-Based Soluble Light-Harvesting CIGS Complex

Yu Chen,*,† Xiaodong Zhuang,† Weian Zhang,*,† Ying Liu,† Ying Lin,† Aixia Yan,*,‡ Yasuyuki Araki,§ and Osamu Ito§

Lab for Advanced Materials, Department of Chemistry, East China University of Science and Technology, 130 Meilong Road, Shanghai 200237, China, State Key Laboratory of Chemical Resource Engineering, Department of Pharmaceutical Engineering, P.O. Box 53, Beijing University of Chemical Technology, 15 BeiSanHuan East Road, Beijing 100029, P. R. China, and Institute of Multidisciplinary Research for Advanced Materials, Tohoku University, Katahira 2-1-1, Sendai 980-8577, Japan

Received May 15, 2007. Revised Manuscript Received July 17, 2007

An easy and versatile solution-based route for the synthesis of a new phthalocyanine-based light-harvesting material PCIGS [Cu_2(*t*Bu_4PcGa)(*t*Bu_4PcIn)S_2TPP_2] is described. This material is prepared through a one-pot reaction of *t*Bu_4PcM-Cl (M = Ga, In), CuI, and $[(CH_3)_3Si]_2S$ in the presence of triphenyl phosphine. In contrast to the dilute solution, the linear absorption coefficient of PCIGS complex in the solid state ($\alpha_0 = 145.35\ cm^{-1}$) is about 150 times greater than the dilute solution ($\alpha_0 = 0.95\ cm^{-1}$) under the conditions of the study. The molecular structure of this material is proposed on the basis of the extended X-ray absorption fine structure spectroscopy.

Introduction

Of all the thin film photovoltaic materials, high-quality CIS ($CuInSe_2$, $CuInS_2$, and $CuGaSe_2$) and CIGS [$Cu(In,Ga)_x(S,Se)_2$] films offer an efficient method of converting solar light into electrical energy and have attracted much attention because of their high absorption coefficient, long-term stability, and low band gap.[1−6] Because of the high cost of production and technical difficulties in the fabrication of large-area cells, there has been a continuing pronounced interest in developing reliable, low-cost, and low-temperature synthetic methods for preparation of CIS and/or CIGS functional materials.[7] The method of CIS and CIGS formation is usually on the basis of vacuum deposition at high temperature over 500 °C. Although electrodeposition from solutions has been used to fabricate relatively low cost CIGS films, stoichiometric control of the product is difficult because of the different rates of Cu, In, Ga, and S(Se) deposition. Hirpo et al. reported the first structurally characterized soluble molecular compounds $(Ph_3P)_2CuIn(QR)_4$ (Q = S,Se; R = ethyl, isobutyl).[8] Cezkeliu and his coworkers prepared a triphenyl phosphite [$(PhO)_3P$] coordinated $CuInS_2$ (CIS) complex in a three-step synthesis using $InCl_3$, CuI, and $[(CH_3)_3Si]_2S$ as starting materials.[9] The resulting deep red solutions were stable against aggregation and oxidation, which allowed further handing in air. Followed Czekeliu's work, Arici et al.[10] incorporated $(PhO)_3P$-stabilized nanoparticles of $CuInS_2$ into polymer matrices to fabricate $CuInS_2$-based hybrid solar cells, which show better photovoltaic response with external quantum efficiencies up to 20%. On the other hand, phthalocyanines have in general relatively longer exciton diffusion lengths (a few hundred nanometers to ∼1 μm), broader absorption bands covering about 50% of the solar spectrum in the solid state, and larger charge-carrier mobility ($0.1-1\ cm^2\ V^{-1}\ s^{-1}$).[11,12] These outstanding properties make them the promising candidates required for the practical organic solar cells. It would thus be very desirable if one can incorporate phthalocyanine into CIGS functional materials to prepare soluble Pc-based CIGS photovoltaic materials (PCIGS). This kind of material will be expected to possess a number of potential advantages over traditional CIGS materials: (1) high solubility in organic

* Corresponding author. E-mail: oematerials@yahoo.com (Y.C.).
† East China University of Science and Technology.
‡ Beijing University of Chemical Technology.
§ Tohoku University.

(1) Gay, R. R. *Sol. Energy Mater. Sol. Cells* **1997**, *47*, 19.
(2) Lisnyak, V. V.; Stus, N. V.; Mariychuk, R. T. *Sol. Energy Mater. Sol. Cells* **2003**, *76*, 553.
(3) Arici, E.; Hope, H.; Schaeffler, F.; Meissner, D.; Malik, M. A.; Sariciftci, N. S. *Appl. Phys. A: Mater. Sci. Process*. **2004**, *79*, 59.
(4) Todorov, T.; Cordoncillo, E.; Sanchez-Royo, J. F.; Carda, J.; Escribano, P. *Chem. Mater*. **2006**, *18*, 3145.
(5) Azulay, D.; Millo, O.; Balberg, I.; Schock, H. W.; Visoly-Fisher, I.; Cahen, D. *Sol. Energy Mater. Sol. Cells* **2007**, *91*, 85.
(6) Delahoy, A. E.; Chen, L.; Sang, B. *Annual Technical Report (15 March 2005−14 March 2006)*; Report NREL/SR-520−40145; National Renewable Energy Laboratory: Golden, CO, 2006; www. nrel.gov.)
(7) (a) Savadogo, O. *Sol. Energy Mater. Sol. Cells* **1998**, *52*, 361. (b) Basol, B. M. *Thin Solid Films* **2000**, 361/362, 514. (c) Probst, V.; Setter, W.; Riedl, W.; Vogt, H.; Wendl, M.; Calwer, H.; Zweigart, S.; Ufert, K. D.; Freienstein, B.; Cerva, H.; Karg, F. H. *Thin Solid Films* **2001**, *387*, 262. (d) Fischer, C. H.; Muffler, H. J.; Baer, M.; Kropp, T.; Schoenmann, A.; Fiechter, S.; Barbar, G.; Lux-Steiner, M. C. *J. Phys. Chem. B* **2003**, *107*, 7516. (e) Kaelin,M.; Rudmann, D.; Kurdesau,F.; Meyer, T.; Zogg, H.; Tiwari, A. N. *Thin Solid Films* **2003**, *431/432*, 58.
(8) Hirpo, W.; Dhingra, S.; Sutorik, A. C.; Kanatzidis, M. G. *J. Am. Chem. Soc*. **1993**, *115*, 1597.
(9) Czekelius, C.; Hilgendorff, M.; Spanhel, L.; Bedja, I.; Lerch, M.; Mueller, G.; Bloeck, U.; Su, D. S.; Giersig, M. *Adv. Mater*. **1999**, *11*, 643.
(10) Arici, E.; Sariciftci, N. S.; Meissner, D. *Adv. Funct. Mater*. **2003**, *13*, 165.
(11) Whitlock, J. B.; Sharma, G. D.; Cox, M. D.; Sauers, R. R.; Bird, G. R. *Opt. Eng*. **1993**, *32*, 1921.
(12) Woehrle, D.; Kreienhoop, L.; Schnurpfeil, G.; Elbe, J.; Tennigkeit, B.; Hiller, S.; Schlettwein, D. J. *J. Mater. Chem*. **1995**, *5*, 1819.

10.1021/cm0713172 CCC: $37.00
Published on Web 10/03/2007

solvents allows the easy manufacture of thin-film devices by spin-coating or screen-printing technologies, which is favorable for reducing the manufacturing cost; and (2) phthalocyanines offer a tremendous degree of design flexibility, so that they may be employed to effectively tune or modify spectral response ranges and optical absorption coefficients of materials. In this contribution, we utilize the chemical reactivity of the M−Cl (M = Ga^{3+}, In^{3+}) bond in the PcM−Cl structure, which allows the preparation of a series of highly soluble axially substituted and/or bridged Pc complexes,[13−15] to prepare the first soluble triphenyl phosphine (TPP)-coordinated PCIGS material (see eq 1).

$$2\mathrm{CuI} + t\mathrm{Bu_4PcInCl} + t\mathrm{Bu_4PcGaCl} + 2[(\mathrm{CH_3})_3\mathrm{Si}]_2\mathrm{S} \xrightarrow[170\ ^\circ\mathrm{C,\ Ar}]{\mathrm{TPP,\ DMA}} \mathrm{Cu_2}(t\mathrm{Bu_4PcIn})(t\mathrm{Bu_4PcGa})\mathrm{S_2TPP_2} + 2(\mathrm{CH_3})_3\mathrm{SiCl} + 2(\mathrm{CH_3})_3\mathrm{SiI} \quad (1)$$

Experimental Section

General. All chemicals were purchased from Aldrich and used without further purification. Organic solvents were purified, dried, and distilled under dry nitrogen. The operations for synthesis prior to the termination reaction were carried out under purified argon. The UV/vis spectral measurements were carried out with a JASCO model V570 DS spectrophotometer. Transmission electron microscopy (TEM) image was recorded on a Hitachi H-800 TEM system operated at 100 kV.

The redox values were measured using the differential pulse voltammetry (DPV) technique by applying BAS CV-50W Voltammetric Analyzer (Japan). A platinum disk electrode was used as working electrode, whereas a platinum wire served as a counter electrode. A Ag/AgCl electrode was used as a reference electrode. All measurements were carried out in different solvents containing 0.1 M tetra-butylammonium percholarate [$(n\text{-Bu})_4\mathrm{NClO_4}$] as a supporting electrolyte at a scan rate of 0.1 V s^{-1}.

Nanosecond-transient absorption measurements were carried out using third harmonic generation (THG, 355 nm) of a Nd:YAG laser (Spectra-Physics, Quanta-Ray GCR-130, 6 ns fwhm) as an excitation source. For transient absorption spectra in the near-IR region (600−1400 nm), monitoring light from a pulsed Xe-lamp was detected with a Ge-avalanche photodiode (Hamamatsu Photonics, B2834). For transient absorption spectra in the visible and near-IR region (400−1000 nm), monitoring light from a pulsed Xe-lamp was detected with a Si−PIN photodiode (Hamamatsu Phonics, S1722−02).

The EXAFS measurements of the compound PCIGS was performed at three edges (i.e., copper K-edge at 8979 eV, gallium K-edge at 10 367 eV and indium K-edge at 27 940 eV) on beamline X1.1 of the Hamburger Synchrotron Radiation Laboratory at DESY, Hamburg, Germany. The compound was measured with a Si(311) double crystal monochromator at the indium K-edge and with a Si(111) double-crystal monochromator at the copper and gallium K-edges. The measurements were carried out under ambient conditions, and ion chambers filled with inert gases (nitrogen and argon) were used to measure the incident and transmitted intensities. A positron energy was 4.45 GeV and the beam current was between 50 and 85 mA. Energy calibration at the copper and indium K-edges was monitored by using 20 μm thick copper and indium metal foils, respectively. A platinum metal foil having an L_{III}-edge at 11 564 eV was used for energy calibration of the gallium K-edge. For solid-state measurements, the compound was embedded in a polyethylene matrix and pressed into a pellet. The concentration of the solid sample was adjusted to yield an extinction of 1.5. Data evaluation started with the removal of background absorption from the experimental spectrum by subtraction of a Victoreen-type polynomial. The spectrum was then convoluted with a series of increasingly broader Gaussian functions, and the common intersection point of the convoluted spectra was taken as energy E_0.[16,17] To determine the smooth part of the spectrum, corrected for preedge absorption, we used a piecewise polynomial. It was adjusted in such a manner that the low-R components of the resulting Fourier transform were minimal. After division of the background-subtracted spectrum by its smooth part, the photon energy was converted into a photoelectron wave vector scale. The resulting EXAFS function was weighted with k^3. Data analysis in k space was performed according to the curved-wave formalism of the program EXCURV92 with the XALPHA phase and amplitude functions.[18] The amplitude factor AFAC was fixed at 0.8, and an overall energy shift (ΔE_0) was introduced to give a best fit to the data. The mean free path of the scattered electrons was calculated from the imaginary part of the potential (VPI, a constant referred to as the Imaginary Potential on the EXAFS Parameters control panel, was set to −4.00 eV. The Imaginary Potential is used to specify experimental broadening: it is a constant that describes the lifetime of the photoelectron and is usually in the range −5 to −1 eV.). In the fitting procedure, the various parameters, i.e., coordination number, interatomic distance, Debye−Waller factor, and energy zero value, were determined by iterations.

Synthesis of PCIGS Complex. To the stirred solution of CuI (190 mg, 1.0 mmol, Aldrich product), $t\mathrm{Bu_4PcGaCl}$ (421 mg, 0.5 mmol), $t\mathrm{Bu_4PcInCl}$ (443.6 mg, 0.5 mmol), and triphenyl phosphine (TPP, 524 mg, 2mmol) in anhydrous *N*,*N*-dimethylacetamide (DMA, 100 mL) was added dropwise an excess of hexamethyldisilathiane (1.78 g, 10 mmol) in DMA over 2 h at 170 °C under argon. After being refluxed at the same temperature for 16 h, the reaction mixture was allowed to cool to room temperature. The solvent was removed by distillation under reduced pressure, leaving a dark green residue that was recrystallized from a mixture of CH_2Cl_2/MeOH (4:3 v/v) by slowly evaporating the more volatile dichloromethane in a rotary evaporator at 40−60 °C under slightly reduced pressure. To complete crystallization, we kept the mixture in a refrigerator overnight. The complex was collected by filtration, washed twice with methanol, and dried at 80 °C in a vacuum. The resultant product was obtained in 72.5% yield (0.86 g).

Results and Discussion

PCIGS complex is highly soluble in common organic solvents, e.g., chlorobenzene, toluene, chloroform, benzene, and tetrahydrofuran, and exhibits a small energy band gap of 1.53 eV (the HOMO/LUMO values measured by electrochemical experiments are −4.85 and 3.32 eV, respectively). The MALDI-TOF mass spectrum of this complex ($C_{132}H_{126}GaInN_{16}Cu_2P_2S_2$, calcd: $m/z = 2374$) shows a peak at $m/z = 2413$, which can be assigned to an ($M^+ + {}^{39}K$) peak. A typical transmission electron microscopy (TEM)

(13) Chen, Y.; Barthel, M.; Seiler, M.; Subramanian, L. R.; Bertagnolli, H.; Hanack, M. *Angew. Chem., Int. Ed.* **2002**, *41*, 3239.
(14) Chen, Y.; Hanack, M.; Araki, Y.; Ito, O. *Chem. Soc. Rev.* **2005**, *34*, 517.
(15) Hanack, M.; Schneider, T.; Barthel, M.; Shirk, J. S.; Flom, S. R.; Pong, R. G. S. *Coord. Chem. Rev.* **2001**, *219/221*, 235.
(16) Ertel, T. S.; Bertagnolli, H.; Hückmann, S.; Kolb, U.; Peter, D. *Appl. Spectrosc.* **1992**, *46*, 690.
(17) Newville, M.; Livins, P.; Yakoby, Y.; Rehr, J. J.; Stern, E. A. *Phys. Rev. B* **1993**, *47*, 14126.
(18) Gurman, S. J.; Binstead, N.; Ross, I. *J. Phys. C* **1986**, *19*, 1845.

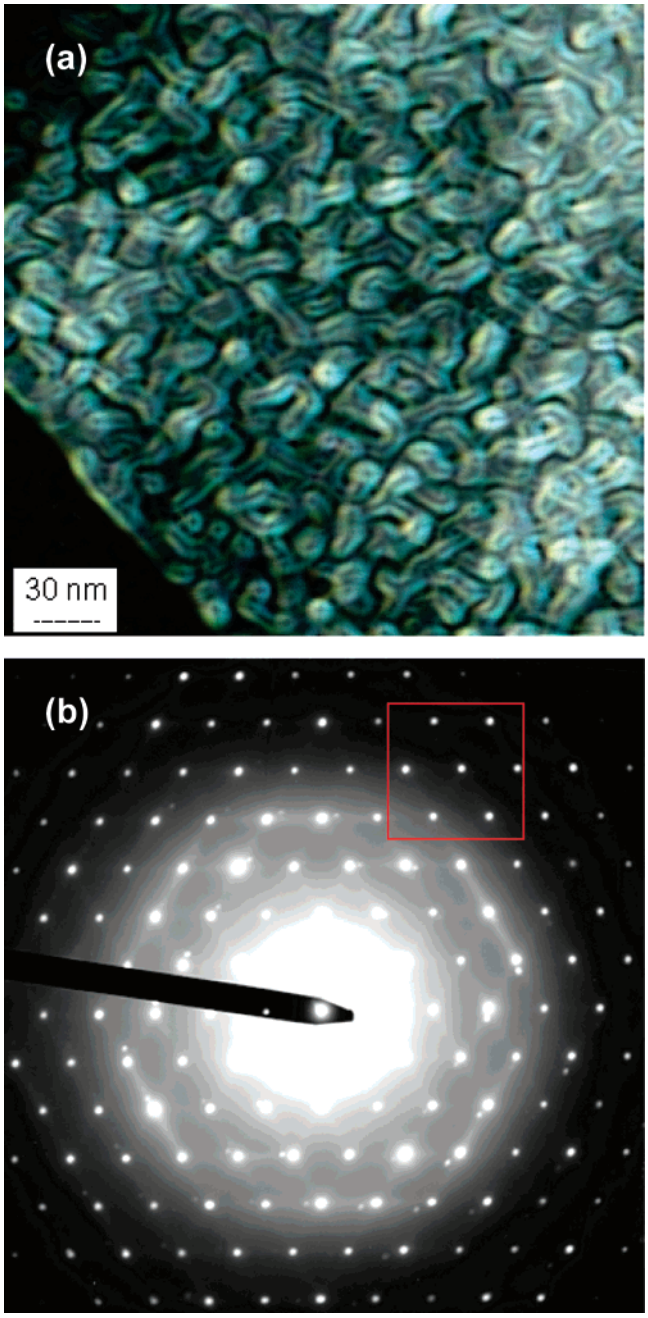

Figure 1. (a) TEM image and (b) electron diffraction pattern of PCIGS complex.

image of the PCIGS is depicted in Figure 1a, where the wormlike geometry of the nanoparticles can be clearly observed. The self-assembly behavior of phthalocyanines and their derivatives[19] has been reported over the past several years. The driving force for this issue in general involves

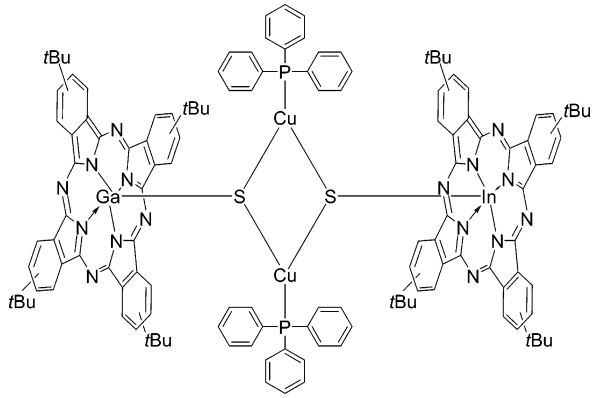

Figure 2. Proposed molecular structure of PCIGS complex.

ligand−metal coordination, $\pi-\pi$ interaction, van der Waals interaction, and donor−acceptor interactions.[20] The formation of the wormlike morphology in this study is due to the ordered stacks of the PCIGS complex, which has been confirmed by the electron diffraction pattern (EDP) displayed in Figure 1b, from which it can be seen that the EDP is composed of hexagonal lattices, suggesting the highly ordered structure of the PCIGS complex, this being quite favorable for the hole and/or electron transportation in the photovoltaic cells. The dark region in the wormlike morphology is perhaps ascribed to the axial part of the stacking PCIGS, whereas the white region maybe corresponds to its organic-rich phase. The proposed molecular structure is shown as Figure 2.

For phthalocyanines, their electronic absorption spectra[21] are characterized by an intense Q-band in the red end of the visible spectrum of light between 600 and 700 nm, with a molar absorption often exceeding 1×10^5 cm^2/mol, and a B-band at 300−400 nm in the blue end of the visible spectrum. In the spectra of metal phthalocyanine solutions, the intense Q-band arises from a doubly degenerate $\pi-\pi^*$ transition between the $A_{1g}(a_{1u}^2)$ ground state to the first excited single state, which has $E_u(a^1_{1u}e^1_g)$ symmetry. The second allowed $\pi-\pi^*$ transition (B-band) is due to a transition between either an a_{2u} or a b_{2u} orbital to the e_g orbital (LUMO). In the spectra of phthalocyanines with open d-shell metal as central atoms, metal to ligand or ligand to metal charge-transfer transitions can be observed.[21] Intermolecular interactions like aggregation give rise to effects like band broadening, shift of the Q- and B-band, or an observed splitting of the Q-band.[22] Figure 3 gives the UV/vis absorption spectra of PCIGS complex. In the chloroform solution (0.005 mM), PCIGS displays a typical electronic absorption spectrum of metal phthalocyanines. The intense absorption bands located at 694 and 620 nm were attributed to the Q-band, whereas the weak band at 339 nm was assigned to

(19) (a) Engelkamp, H.; Middelbeek, S.; Nolte, R. J. M. *Science* **1999**, *284*, 785. (b) Kobayashi, N. *Coord. Chem. Rev.* **2001**, *219/221*, 99; (c) George, S. J.; Ajayaghosh, A. *Chem.—Eur. J.* **2005**, *11*, 3217.

(20) (a) Hunter, C. A.; Sanders, J. K. M. *J. Am. Chem. Soc.* **1990**, *112*, 5525. (b) Duro, J. A.; de la Torre, G.; Torres, T. *Tetrahedron Lett.* **1995**, *36*, 8079. (c) Schutte, W. J.; Sluyters-Rehbach, M.; Sluyters, J. H. *J. Phys. Chem.* **1993**, *97*, 6069. (d) Hanack, M.; Hirsch, A.; Lehmann, H. *Angew. Chem., Int. Ed.* **1990**, *29*, 1467. (e) Martinez-Diaz, M. V.; Rodriguez-Morgade, M. S.; Feiters, M. C.; van Kan, P. J. M.; Nolte, R. J. M.; Stoddart, J. F.; Torres, T. *Org. Lett.* **2000**, *2*, 1057. (f) de la Escosura, A.; Mart'nez-D'az, M. V.; Thordarson, P.; Rowan, A. E.; Nolte, R. J. M.; Torres, T. *J. Am. Chem. Soc.* **2003**, *125*, 12300.

(21) (a) Chen, Y.; Hanack, M.; Blau, W. J.; Dini, D.; Doyle, J.; Liu, Y.; Lin, Y.; Bai, J. *J. Mater. Sci.* **2006**, *41*, 2169. (b) Heckmann H. Ph.D. Thesis, University of Tübingen, Tübingen, Germany, 1999. (c) Stillman, M. J.; Thomson, A. J. *J. Chem. Soc., Faraday Trans. 2* **1974**, *70*, 790.

(22) (a) George, R. D.; Snow, A. W.; Shirk, J. S.; Barger, W. R. *J. Porphyrins Phthalocyanines* **1998**, *2*, 1. (b) Hollebone, B. R.; Stillman, M. J. *J. Chem. Soc., Faraday Trans. 2* **1978**, *74*, 2107. (c) Dodsworth, E. S.; Lever, A. B. P.; Seymour, P.; Leznoff, C. C. *J. Phys. Chem.* **1985**, *89*, 5698. (d) Schutte, W. J.; Sluyters-Rehbach, M.; Sluyters, J. H. *J. Phys. Chem.* **1993**, *97*, 6069.

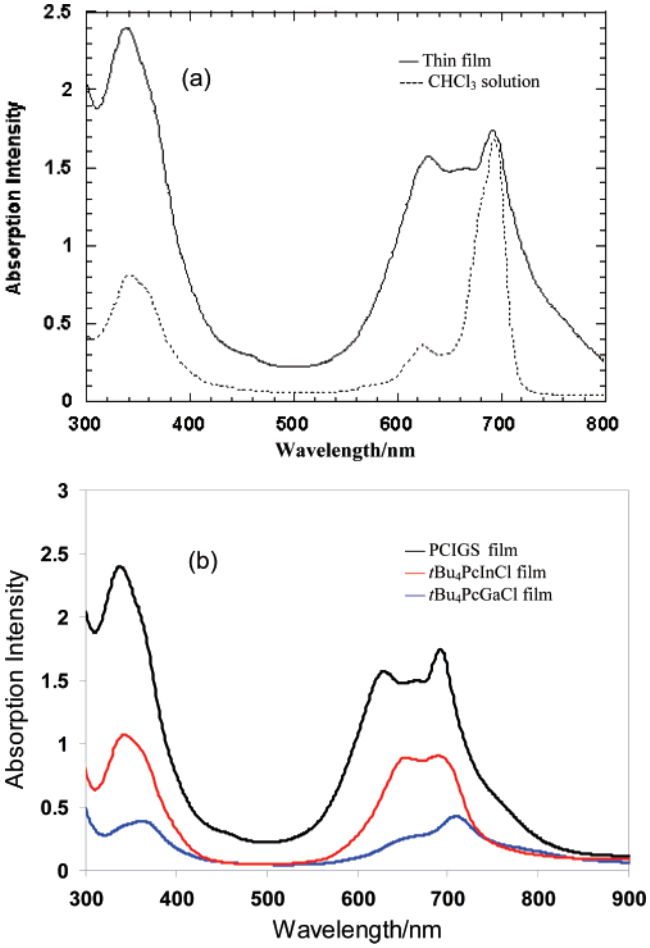

Figure 3. UV/vis absorption spectra of (a) PCIGS in thin film and in $CHCl_3$ solution (0.005 mM), and (b) PCIGS, *t*Bu_4PcInCl, and *t*Bu_4PcGaCl thin films.

the B-band. In contrast to the dilute solution, the linear absorption coefficient of PCIGS complex in the solid state ($\alpha_0 = 145.35$ cm^{-1}) is about a factor of 150 greater than that for the same molecule in the dilute solution ($\alpha_0 = 0.95$ cm^{-1}) under the conditions of the study. The absorption in the thin film spectrum is broader compared to the solution spectrum. The Q-band in the thin film includes a wing beyond 800 nm on the red side of the Q-band, indicative of aggregated behavior, which is expected because of the large concentration of about 6 g/L that was used in the film construction and the fact that the solid state is naturally more condensed. When compared to the peak at 694 nm, the absorption intensity of the peak at 620 nm increases significantly in the film spectrum, followed by the appearance of a new absorption peak at 662 nm. From the thin film spectra of the starting materials *t*Bu_4PcInCl and *t*Bu_4PcGaCl (Figure 3b), we did not observe this new peak, implying that this peak may be associated with the bridged axial ligands between two Pc macrocycles. Upon excitation with nanosecond laser pulse at 355 nm, i.e., roughly at the center of the B-band, the transient absorption spectrum of PCIGS in toluene (Figure 4) was observed in argon-saturated anhydrous toluene. The transient absorption band appeared at ca. 500 nm after the laser pulse irradiation is attributed to the triplet−triplet absorption of the phthalocyanine compounds.[12,13] The presence of oxygen gives rise to the acceleration of the decay

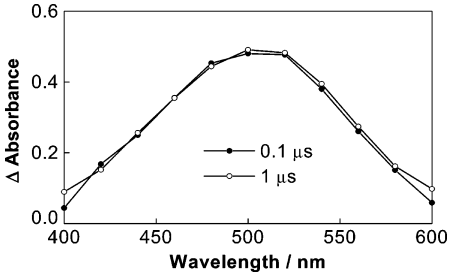

Figure 4. Nanosecond transient absorption spectra of PCIGS complex (0.05 mM) in argon-saturated toluene.

for the absorption band centered at 500 nm. This would indicate the quenching of Pc's triplet state by oxygen. In the absence of oxygen, the decay rates depend on the laser powers.

It is known that the disadvantage of peripherally unsubstituted phthalocyanines is their poor solubility in organic solvents. To overcome this problem, a variety of substituents, for example, alkoxy, alkyl, aryl, F, CF_3, and others, have been attached to the macrocycle, in varying numbers and different substitution patterns.[14] In comparison with octa-substituted phthalocyanine, tetrasubstituted phthalocyanine exhibits the much higher solubility, mainly because of a lower degree of order in the solid state, which facilitates solvation by the more pronounced interaction with solvent molecules. Also, the less symmetric isomers possess a higher dipole moment caused by the more asymmetric arrangement of the substituents in the periphery of the macrocycle. Tetra-(*tert*-butyl)-substituted Pcs and their metal complexes are the most frequently used when solubility is required. This is the reason why we chose tetra(*tert*-butyl)-substituted Pcs as starting materials in the synthesis of PCIGS complex. Hanack and his co-workers[23] were the first to separate the four isomers of tetrasubstituted Pcs and to undertake careful, detailed, and extensive NMR studies probing the influence of isomers on the NMR spectra of the Pcs. The NMR spectrum of an isomeric mixture is only somewhat different from the pure isomers, but it is still possible to draw definite conclusions about the structure. Like most of the peripherally substituted phthalocyanines, PCIGS could not be obtained as a single crystal for an X-ray structural determination. If the octasubstituted phthalocyanine was used as the synthetic precursor, the single-crystal could be theoretically obtained. However, in this case, the solubility of the resultant product is too low to be further processed. In such cases, transmission extended X-ray absorption fine structure (EXAFS) spectroscopy is considered to be a powerful technique for the determination of local structure of a specific atom, regardless of the state of the sample. EXAFS provides information on the coordination number, the nature of the scattering atoms surrounding the absorbing atom, the interatomic distance between the absorbing atom and the backscattering atoms, and the Debye−Waller factor, which accounts for the disorders due to static displacements and thermal vibrations.[24,25]

(23) Sommerauer, M.; Rager, C.; Hanack, M. *J. Am. Chem. Soc.* **1996**, *118*, 10085.
(24) Krishnan, V.; Feth, M. P.; Wendel, E.; Chen, Y.; Hanack, M.; Bertagnolli, H. *Z. Phys. Chem.* **2004**, *218*, 1.

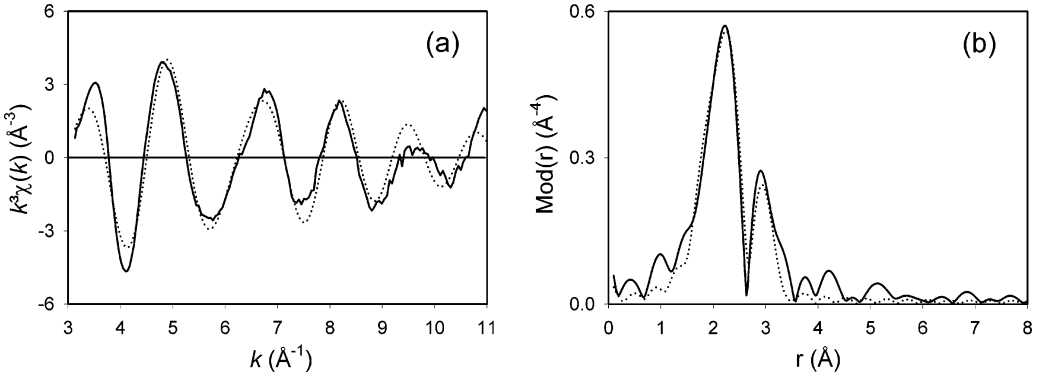

Figure 5. Experimental (solid line) and calculated (dotted line) EXAFS functions and their corresponding Fourier transforms of PCIGS measured at Cu K-edge.

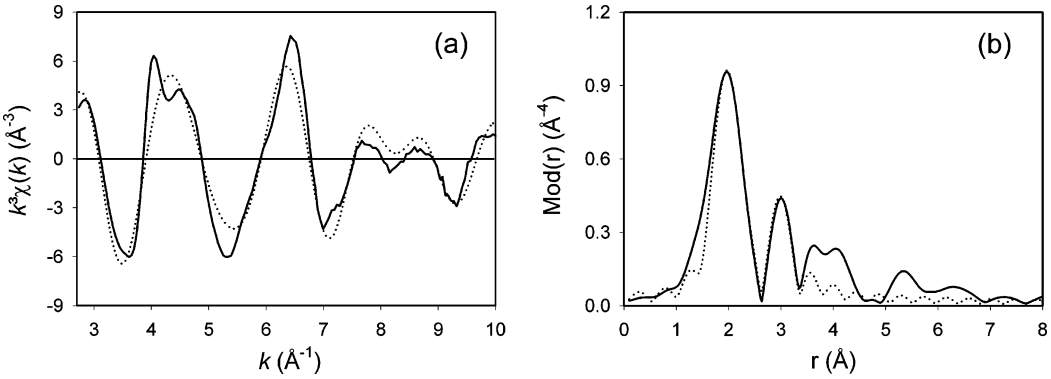

Figure 6. Experimental (solid line) and calculated (dotted line) EXAFS functions and their corresponding Fourier transforms of PCIGS measured at Ga K-edge.

Table 1. EXAFS Determined Structural Data for PCIGS Measured at Cu K-Edge

A−Bs[a]	N[b]	r^c (Å)	σ^d (Å)	$\Delta E_0{}^e$ (eV)	*k*-range (Å^{-1})	fit-index
Cu−S	2.3 ± 0.2	2.15 ± 0.02	0.105 ± 0.011	19.75	3.1−11.0	33.56
Cu−P	1.0 ± 0.1	2.32 ± 0.02	0.055 ± 0.006			
Cu−Cu	1.4 ± 0.2	2.82 ± 0.03	0.105 ± 0.013			

[a] Absorber−backscatterers. [b] Coordination number. [c] Interatomic distance. [d] Debye−Waller factor σ with its calculated deviation. [e] Shift of the threshold energy ΔE_0.

Table 2. EXAFS Determined Structural Data for PCIGS Measured at Ga K-Edge

A−Bs[a]	N[b]	r^c (Å)	σ^d (Å)	$\Delta E_0{}^e$ (eV)	*k*-range (Å^{-1})	fit-index
Ga−N_{Indol}	4.1 ± 0.4	2.00 ± 0.02	0.071 ± 0.007	15.47	2.7−10.0	32.77
Ga−C	8.4 ± 0.8	3.01 ± 0.03	0.089 ± 0.010			
Ga−N_{Aza}	3.7 ± 0.4	3.30 ± 0.04	0.110 ± 0.013			
Ga−S	1.0 ± 0.1	2.33 ± 0.02	0.081 ± 0.010			

[a] Absorber−backscatterers. [b] Coordination number. [c] Interatomic distance. [d] Debye−Waller factor σ with its calculated deviation. [e] Shift of the threshold energy ΔE_0.

The experimentally determined and fitted EXAFS functions of PCIGS measured at copper K-edge are shown in *k*-space as well as by Fourier transforms in real space in Figure 5. The structural parameters are summarized in Table 1. In the analysis of the experimental k^3 weighed $\chi(k)$ function, a three-shell model can be fitted for the measurements performed at the copper K-edge. The first shell having about two sulfur backscatterers was found at about 2.15 Å distance. The determined copper−sulfur distance is in agreement with those reported for CuS.[26,27] The second shell with about one phosphorus backscatterer was fitted at about a 2.32 Å distance. For comparison, the reported copper−phosphorus distances are 2.28 Å for $(PPh_3)_2CuIn(SEt)_4$[8] and 2.24 Å for $Cu_6In_8Se_{13}Cl_4(PPh_3)_6(C_4H_8O)$.[28] An additional shell consisting of a copper backscatterer was determined at about 2.82 Å distance. The direct coordination of gallium or indium with copper was not evidenced from the EXAFS evaluation.

The experimentally determined and fitted EXAFS functions of PCIGS measured at gallium K-edge are shown in *k*-space as well as by Fourier transforms in real space in Figure 6 and the corresponding structural parameters are given in Table 2. The analysis of the data shows the contribution of phthalocyanine macrocycle in the spectra. In agreement with the well-known structure of phthalocyanine complexes, about four nitrogen backscatterers at 2.00

(25) Lytle, F. W.; Sayers, D. E.; Stern, E. A. *Phys. Rev. B* **1975**, *11*, 4825.
(26) Takeuchi, Y.; Kudoh, Y.; Sato, G. *Z. Kristallogr.* **1985**, *173*, 119.
(27) Gotsis, H. J.; Barnes, A. C.; Strange, P. *J. Phys. Condens. Matter* **1993**, *4*, 10461.
(28) Eichhöfer, A.; Fenske, D. *J. Chem. Soc., Dalton Trans.* **2000**, 941.

Å, arising from the indol nitrogen atoms, and another four nitrogen backscatterers at 3.30 Å, stemming from the aza nitrogen atoms, were found. In addition, another shell consisting of about eight carbon backscatterers at 3.01 Å was observed. All these distances can be assigned to intramolecular contributions.[29] Besides the expected three shells of the phthalocyanine macrocycle, a significant improvement in the fit index was obtained by considering a sulfur backscatterer at a distance of 2.33 Å in the evaluation of the spectrum. The determined distance is in very good agreement with reported gallium−sulfur distances of 2.33 Å for GaS[30] and 2.32 Å for Ga_2S_3.[31] The feature at about 4 Å is likely due to eight carbon backscatterers in the phthalocyanine macrocycle.[32,33] A fitting with this backscatterer in this distance range does not increase the agreement of the experimental EXAFS function compared to the fitted function, and hence, this shell was not considered for evaluation. In the Ga K-edge EXAFS analysis as well, the gallium−copper interactions could not be evidenced.

The EXAFS measurements performed at In K-edge could not be evaluated because of the very bad signal-to-noise ratio in the measured spectrum. It is supposed that the indium phthalocyanine subunit has coordination geometry similar to that of its gallium counterpart in PCIGS molecule. This argument is further supported by the absence of copper−indium interactions from the Cu K-edge measurements. On the basis of this postulation and the EXAFS analysis at the copper and gallium K-edges, the proposed molecular structure of PCIGS is shown in Figure 2. This finding can also be partially supported by the single-crystal structural data of $(Ph_3P)_2CuIn(QR)_4$,[8] which feature tetrahedrally coordinated indium and copper atoms bridged by thio(seleno)lates forming a planar "$CuIn(QR)_4$" core, the terminal ligands are two phosphines on the Cu and two thiolates or selenolates on the indium atom.

In summary, the first phthalocyanine-based soluble CIGS complex (PCIGS) was synthesized by one-pot reaction of CuI, tBu$_4$PcGaCl, tBu$_4$PcInCl, and hexamethyldisilathiane in the presence of triphenyl phosphine at 170 °C. The linear absorption coefficient of PCIGS complex in the solid state ($\alpha_0 = 145.35\ cm^{-1}$) is about 150 times greater than the dilute solution ($\alpha_0 = 0.95\ cm^{-1}$) under the conditions of the study. The molecular structure of the PCIGS complex is proposed on the basis of the EXAFS analysis. Further studies on the photophysical and photovoltaic properties of this material are being planned.

Acknowledgment. We are grateful for the financial support of the National Natural Science Foundation of China (20546002, 20676034), ECUST (YJ0142124), China/Ireland Science and Technology Collaboration Research Foundation (CI-2004-06), New Century Excellent Talents in University (NCET-050413), Shanghai Municipal Educational Commission (SMEC-05SG35), and Science and Technology Commission of Shanghai Municipality (STCSM-05XD14004), respectively. We also express our thanks to Mr. Krishnan for the EXAFS measurements and data analysis on the PCIGS complex.

CM0713172

(29) Vogt, L. H.; Zalkin, A.; Templeton, D. H. Jr. *Inorg. Chem.* **1967**, *6*, 1725.
(30) Kuhn, A.; Chevy, A. *Acta Crys. B* **1976**, *32*, 983.
(31) Jones, C. Y.; Bryan, J. C.; Kirschbaum, K.; Edwards, J. G. *Z. Krist. New Cryst. Struct.* **2001**, *216*, 327.
(32) Weber, A.; Ertel, T. S.; Reinöhl, U.; Feth, M.; Bertagnolli, H.; Leuze, M.; Hanack, M. *Eur. J. Inorg. Chem.* **2001**, 679.
(33) Bertagnolli, H.; Weber, A.; Hörner, W.; Ertel, T. S.; Reinöhl, U.; Hanack, M.; Hees, M.; Polley, R. *Inorg. Chem.* **1997**, *36*, 6397.